Power System Protection and Control
ISSN:1674-3415

HIGH-FIDELITY SOLAR SUNSPOT IMAGE DENOISING: A COMPARATIVE ANALYSIS OF ADAPTIVE ANISOTROPIC DIFFUSION, NON-LOCAL MEANS, AND HYBRID FILTERING APPROACHES

Nagarathna H S[1], Goutham M A[2]

[1]Department of Electronics and Communication Engineering ,Dr.Ambedkar Institute of Technology,Bengaluru-560056, Karnataka,India ,nagarathnahs.ec@drait.edu.in
[2]Department of Electronics and Communication Engineering,Adichunchanagiri Institute of Technology,Chikkamagaluru - 577102, Karnataka, India , magoutham@gmail.com

Received: 22/04/2026 **Revised**: 22/05/2026 **Accepted**: 27/06/2026

ABSTRACT:

Solar image denoising plays a critical role in enhancing sunspot detection accuracy, solar activity monitoring, and the predictive capabilities of space weather models. Nevertheless, data captured by solar observatories are often corrupted by various forms of degradation, including sensor, photon, and speckle noise, as well as instrumental artifacts, which collectively diminish image fidelity and hinder automated analysis pipelines. To mitigate these issues, this research evaluates three distinct denoising strategies: Adaptive Anisotropic Diffusion, Non-Local Means, and a hybrid AAD+NLM approach. By integrating AAD's edge-preserving diffusion capabilities with NLM's non-local similarity analysis, the proposed hybrid framework achieves superior noise suppression while maintaining critical structural features. The effectiveness of these methodologies was assessed utilizing SDO/HMI, AIA 171 Å, and AIA 193 Å datasets, with performance evaluated through metrics such as Peak Signal-to-Noise Ratio, Structural Similarity Index, Mean Squared Error, Edge Preservation Index, and computational efficiency. Experimental findings indicate that the hybrid approach yields superior denoising performance and enhanced structural integrity, resulting in more robust sunspot visualization and confirming its efficacy for automated solar image analysis.

Keywords*: Adaptive Anisotropic Diffusion(AAD), Non-Local Means(NLM), hybrid AAD+NLM,SDO/HMI, AIA 171 Å, and AIA 193 Å,PSNR,SSIM.*

INTRODUCTION

The Sun is a massive star considered the center of our solar system. The Sun is made of plasma, and because of its motion, the magnetic field lines around the Sun become twisted, bent, or tangled. The magnetic flux concentration inhibits heat transfer to the solar surface, leading to the formation of dark, cool areas on the Sun called sunspots. Accurate identification and characterization of sunspots are very important because they play a key role in developing effective space weather monitors. However, the intrinsic noise within solar images makes it difficult to extract accurate data on sunspots. Accurate sunspot detection, segmentation, and extraction will significantly enhance our ability to conduct research into solar physics and to predict weather in outer space. Space-based telescopes such as SOHO and SDO capture high-quality images of the Sun because they are free of atmospheric turbulence, but there are many noise sources that affect the quality of the images obtained by these telescopes (including speckle and granular noise). These sources of noise will degrade image quality, making it necessary to apply effective denoising techniques to improve the quality of the solar images used for these purposes. Many traditional image processing algorithms struggle to produce clear full-disk solar images due to the extreme dynamic range and contrast. Thus, state-of-the-art denoising techniques must be applied to solar images to significantly enhance their quality for research purposes.

Although solar observatories like SOHO and SDO avoid the atmospheric distortion inherent in ground-based systems, their images remain susceptible to degradation from instrumental limitations and adverse space conditions, introducing noise that can hinder accurate sunspot detection and characterization. The deep learning model for solar image segmentation presented here is trained on solar image data to learn discriminative representations. Traditional sunspot analysis typically relies on hand-crafted features—such as area, intensity

 DOI: 10.46121/pspc.54.3.05

contrast, and geometric characteristics—which are often susceptible to brightness fluctuations, limb darkening, and granulation noise. Furthermore, even in the absence of external disturbances, raw SOHO and SDO images frequently exhibit inherent granular distortions and speckle noise.

Anisotropic diffusion (AD) is an edge-preserving method for reducing noise in images and smoothing the resulting image while preserving some of the more important features or structures, such as sunspot boundaries (You et al. 1996). Bourgeois et al. (2024) applied AD and mathematical morphology to SDO/HMI images, thereby improving sunspot detection and sunspot area estimation. The non-local means (NLM) method reduces noise by exploiting the self-similarity of image data within an image, resulting in much better preservation of image structure than most traditional filtering techniques (Buades et al., 2007). Zhang et al. (2022), Fang et al. (2022), and Kong et al. (2024) proposed modifications to NLM that improve its denoising capability by using adaptively selected parameters, statistical measures of similarity, and gradient-based weighting schemes. The hybrid denoising methods that combine NLM with other filtering techniques are also demonstrating good results. Taassori and Vízvári (2024) designed an integrated adaptive Kalman filter, NLM, and median filter method to effectively reduce noise while preserving image detail. Gor and Bhensdadia (2024) used an NLM and wavelet transform, combined with deep learning models, to achieve high PSNR and SSIM values.

Recent work in restoration via imaging will see great advances due to improvements such as enhancements using Deep Learning techniques including CNNs, GANs, and Denoising Diffusion Probabilistic Models (DDPMs) that are far superior to traditional restoration methods for denoising and will require a significant amount of images as per AIA for imaging Solar system images, however very little research has been done to compare either Adaptive Anisotropic Diffusion (AAD) or Non-Local Means (NLM) to Hybrid (AAD+ NLM) filter techniques as methods used specifically for Denosing solar imagery. This research will look at evaluating these methods against one another by utilizing image quality measurements and features preservation measures to compare the efficiencies of each technique in terms of utilizing SDO imagery and quantifying the efficiency of each denoised image technique against each technique's ability to preserve solar hemisphere data, such as sunspot borders and textural characteristics as a reference to providing accurate information for reliable detection of solar weather analysis.
The goal of this research is to develop an inexpensive denoising framework to enhance the ability to detect and study solar activity. Solar images obtained from ground- and space-based observatories typically contain a large amount of sensor noise, as well as atmospheric distortion, uneven brightness, limb darkening, and bright active areas, and reduced contrast, which makes it very difficult to see specific features with the naked eye and or cause automatic detection and segmentation systems to produce inaccurate results.In order to address this problem, we tested three different denoising methods (Adaptive Anisotropic Denoising (AAD), Non-Local Means (NLM) and the Hybrid (AAD+NLM) filtering approaches) as well as several preprocessing techniques (image normalization, enhancement of brightness and contrast, and correction of limb darkening) to equalize the intensity throughout the entire solar disc, hence reducing the degree of intensity variance in order to make the solar features more visible, before being denoised.

Filtering methods were investigated using Peak Signal-to-Noise Ratio (PSNR), Structural Similarity Index Measure (SSIM), Mean Squared Error (MSE), edge correlation, texture correlation, and calculation time. Determining which filter has the best rank in reducing noise, preserving edges, preserving texture, and remaining computationally efficient will depend on selecting the filter that preserves solar features, such as the boundaries of sunspots, umbrae, penumbrae, and other small features, so that data can be accurately evaluated and analyzed. The hybrid technology described in this study differs from traditional smoothing methods in that it uses both true smoothing methods and combines them to produce less noise while maintaining the integrity of the data's structure, leading to high-quality images with clear features. Therefore, using a hybrid approach to generate images of the sun yields an excellent representation of its features and provides high-quality information for extracting and segmenting them, compared with results from traditional smoothing techniques. This improved hybrid technique will enable more accurate detection of sunspots and provide better tools for monitoring the sun and developing accurate space weather forecasts.

ADAPTIVE ANISOTROPIC DIFFUSION FILTER

High-resolution solar images from space- and ground-based sources (such as SOHO, SDO, or ground solar telescopes) are often affected by various types of noise, including CCD electronic noise, photon (shot) noise, and noise from granulation and atmospheric/instrumental effects. While traditional linear filtering has been used to remove noise from solar images, it often also blurs important solar features, including the boundaries of sunspots, umbra–penumbra transitions, and magnetic discontinuities.

A nonlinear PDE-based approach (AAD) that employs PDEs for Adaptive Anisotropic Diffusion (AAD) filtering allows us to circumvent this restriction. AAD filtering preserves (and possibly enhances) edges while smoothing homogeneous regions of the image. Figure 6.1 also depicts the AAD pipeline for pre-processing solar images, which serves as a comprehensive adaptive anisotropic diffusion (AAD) process (or "pipeline") for acquiring solar images.

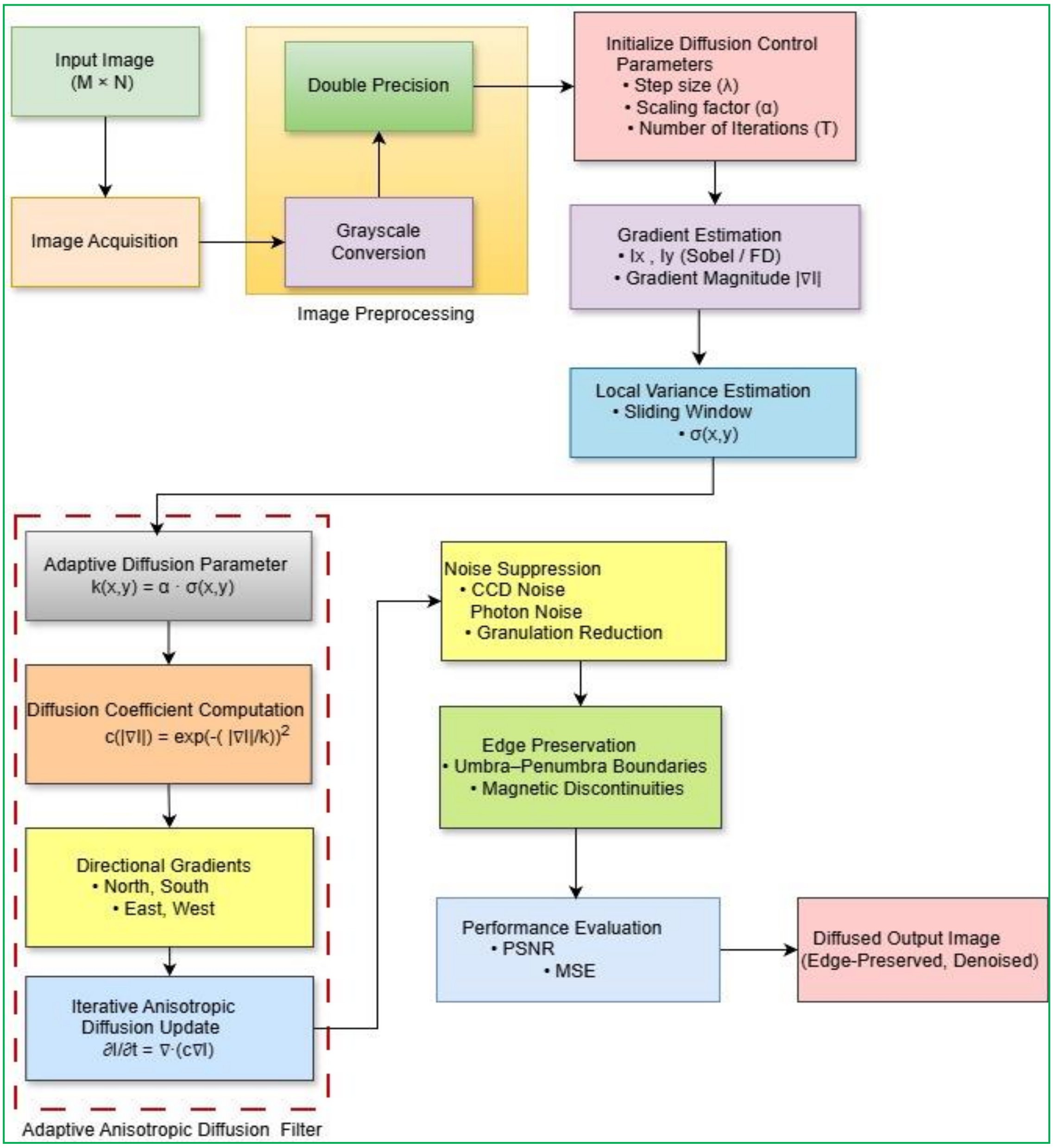

Figure 2.1: Adaptive antistrophic diffusion filter model

Resizing an image taken by an observatory is the initial stage. Because of their creation, these images will typically exhibit non-uniform sensor artifacts (e.g., quantization and statistical variance from photon noise). After the image has undergone several calibration procedures, including flat-field correction and dark-frame subtraction to eliminate sensor-related artifacts, the acquisition is considered complete. Calibration procedures are crucial for

Power System Protection and Control
ISSN:1674-3415

maintaining the authenticity of images taken from the sun so they can be used for additional scientific analysis, although they are typically not shown in a processing diagram Figure 2 .1.

The next step in the process is image pre-processing, which provides numerical stability and consistency before moving on to the diffusion technique once RGB or multispectral solar images have been converted to grayscale. This enables more effective image processing, as the intensity of grayscale images can be used to predict the extent of anisotropic diffusion. We will do this during preprocessing so that the boundaries of sunspots and other features on the sun's surface won't be lost when converting to grayscale. After converting an image (to grayscale), you must convert it to double (or higher) precision from an 8-bit format. When solving diffusion equations and performing numerous numerical iterative updates, you will require this level of precision when calculating gradient vectors. When performing iterative diffusion calculations, it is recommended that you use double (or higher) precision data types to help reduce rounding errors and provide more stability in your results.

The diffusion control parameters are set after preprocessing. The chosen parameters that determine the behavior and efficiency of the diffusion process are the foundation of adaptive anisotropic diffusion. The scaling factor (α) is used to regulate the extent to which the diffusion process is sensitive to local intensity differences in the image. The increment of diffusion in each iteration is determined by the time step size (Δt), which should be small to ensure numerical stability. The number of iterations (T) is the amount of smoothing applied to the image. This can be enhanced by increasing the number of iterations, though too many can lead to over-smoothing and the loss of valuable features. The strength and dynamics of image evolution in diffusion are controlled by these parameters in combination.

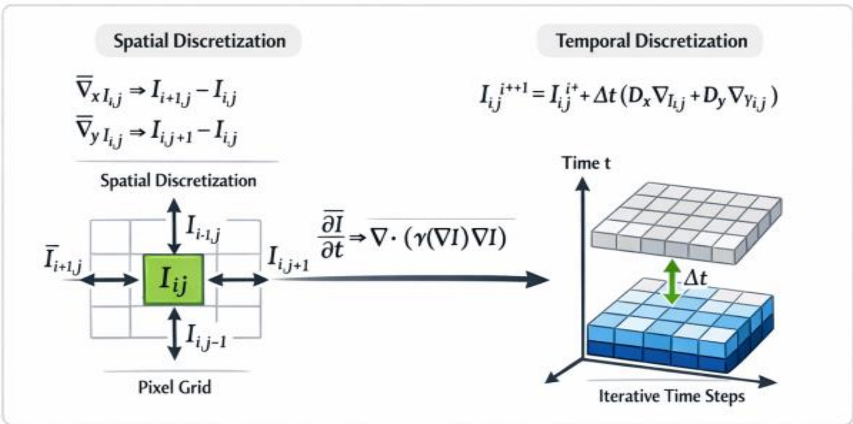

Figure 2.2 Discretization of the PDE for Anisotropic Diffusion

The second step is to estimate gradients, which is critical for identifying edges in the picture. Typically, spatial gradients along both the horizontal and vertical axes (Ix and Iy) are computed using operators such as the Sobel filter and finite difference methods as shown in Figure 2.2. The gradient magnitude (|∇I|), which identifies where local intensity changes have occurred, is calculated using the gradients computed above; the greater the gradient magnitude, the more pronounced the edge (or boundary) (e.g., sunspot boundary); the smaller the gradient magnitude, the less variation in intensity occurs over the region.Finally, local variance estimation is done to present adaptive behavior to the diffusion process. Adaptive anisotropic diffusion, unlike classical anisotropic diffusion, uses local statistical data to improve denoising performance. A sliding-window approach is used to compute the local variance $\sigma^2(x, y)$ for each pixel. This variance indicates the local texture and noise properties of the image. High-variance regions are usually associated with edges or intricate solar structures, while low-variance regions are smooth. The diffusion process can modify its behavior by region using this information about local variance. It will be stronger in homogeneous regions and weaker in regions with significant structural features, such as sunspot boundaries.

NON-LOCAL MEANS (NLM)

The algorithm shown in Figure 3.1 automatically finds and segments sunspots in grayscale images of the solar disk. This is accomplished using an adaptive preprocessing-spatio-temporal segmentation approach.Input images may contain various types of contamination that can obscure the presence of sunspots, including sensor noise, uneven illumination, and low-frequency texture variations on the photosphere. Therefore, it is advantageous to estimate the noise level by selecting a small section of the image that is free of other stable data. By measuring the noise level in this section, noise suppression can be applied when processing other portions of the picture. Assessing the amount of noise in the image will allow an appropriate level of noise reduction while preserving significant image structures. The output from this noise-guided preprocessing stage provides a suitably processed image for better analysis in subsequent steps.

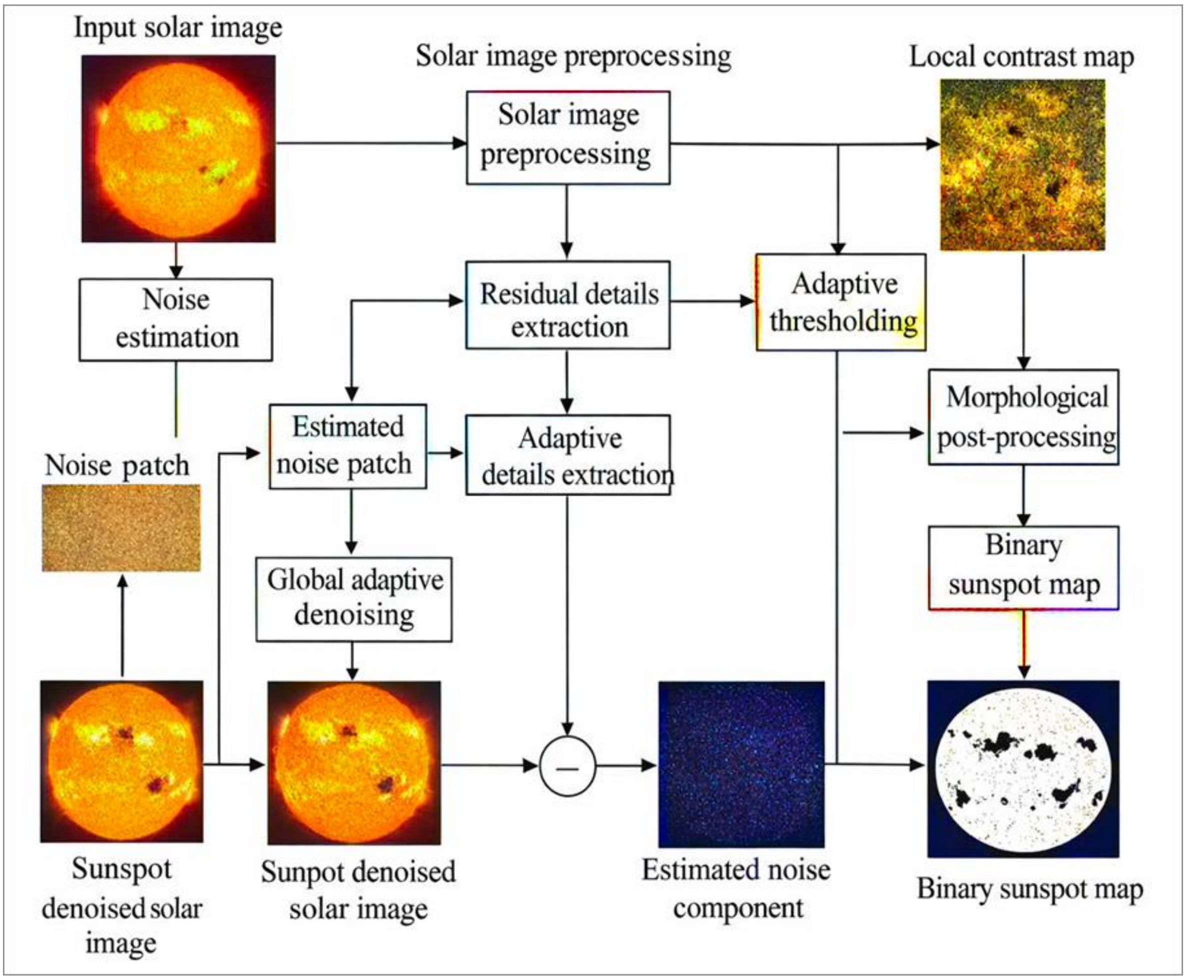

Figure. 3.1. Non-Local Means (NLM) model.

The Steps taken to prep the solar image include negating the image to continue the analysis. Normalizing brightness makes it easier to see dark areas (such as sunspots) because brightness is uniform across the solar disk. This normalizes the image contrast. The naked image may also be slightly smoothed to reduce high-frequency variations while preserving necessary edge information. Accurate feature extraction and segmentation of the solar image are made possible by the enhancement of a properly preprocessed image. The next step to improve the clarity of sunspot features is to denoise the preprocessed image.

The final step of the denoising process is to denoise the original image using an adaptive global denoising method that relies on predicted noise parameters. In contrast to static (fixed-parameter) denoising methods, which apply a fixed level of noise reduction to each image, the adaptive denoising method varies the level of denoising for each original image based on the amount of noise detected in that image. This ensures that, when the denoised image is created, the background remains smooth while retaining the sunspot boundaries. The final denoised product will have a background with a clean solar surface, with features that stand out more prominently than in the original image, as the amount of denoising is determined by the original image's characteristics. To identify features removed by denoising, the denoised image is subtracted from the original image before preprocessing (before denoising). By applying this denoising process to the original image, dark sunspots will contrast more

DOI: 10.46121/pspc.54.3.05

sharply with the bright solar background than they did in the original, thereby enhancing their visibility. To better differentiate sunspots from solar textures, an adaptive feature-extraction method is used to increase local contrast and enhance feature differentiation. A local contrast map is generated for each pixel in the final denoised image, showing the contrast (or contrast intensity) at that pixel. As a result, sunspots appear as zones of very low contrast compared to the surrounding photosphere.

Morphological processing techniques - including opening, closing, and area filtering - will be employed as a post-processing operation to refine the segmentation results. These techniques will reduce the number of isolated noise pixels, fill holes located inside sunspot regions, and smooth edges around objects. Other techniques that filter out insignificant artifacts based on area will yield a clean binary sunspot map for later analysis. The object-oriented framework described earlier was created as a comprehensive tool for detecting sunspots, using adaptive noise estimation, adaptive noise suppression, differential enhancement, contrast-based segmentation, and morphological enhancements, all performed in an integrated fashion. It will provide users with a consistent and reliable method for detecting sunspots regardless of the amount and type of noise present during image capture, as well as the lighting conditions under which the image may have been captured. To objectively demonstrate the performance of the proposed method, we will perform comparisons against several competing NLM-based methods as well as across state-of-the-art denoising algorithms on both standard test images and real images that have been degraded by either Gaussian noise or speckle noise. Objective and qualitative evaluations demonstrate that the proposed method achieves superior performance in noise removal and detail preservation compared to existing techniques.

HYBRID FILTER APPROACH (AAD+NLM)

AAD and NLM differ as methods of denoising an image. AAD uses a PDE-based method that reduces noise by smoothing the image while preventing diffusion at the edges. This is important in solar images, as AAD preserves essential features, like sunspot edges. Further, AAD is a local process.Non-Local Means filtering averages similar patches across the entire image, rather than just pixels within the filter window. Because Non-Local Means is a non-local filter, it does a better job than traditional local filtering methods of preserving image texture and structure at a finer scale. Because of how Non-Local Means operates, it will require more resources and take longer to search for and compare similar patches across the entire image than a traditional local filter would.

For sunspot image analysis, AAD is a better choice than NLM because it processes the image faster and requires less edge deletion. In contrast, when using the same data for the same task, NLM will provide the best texture retention and will give the greatest noise reduction.

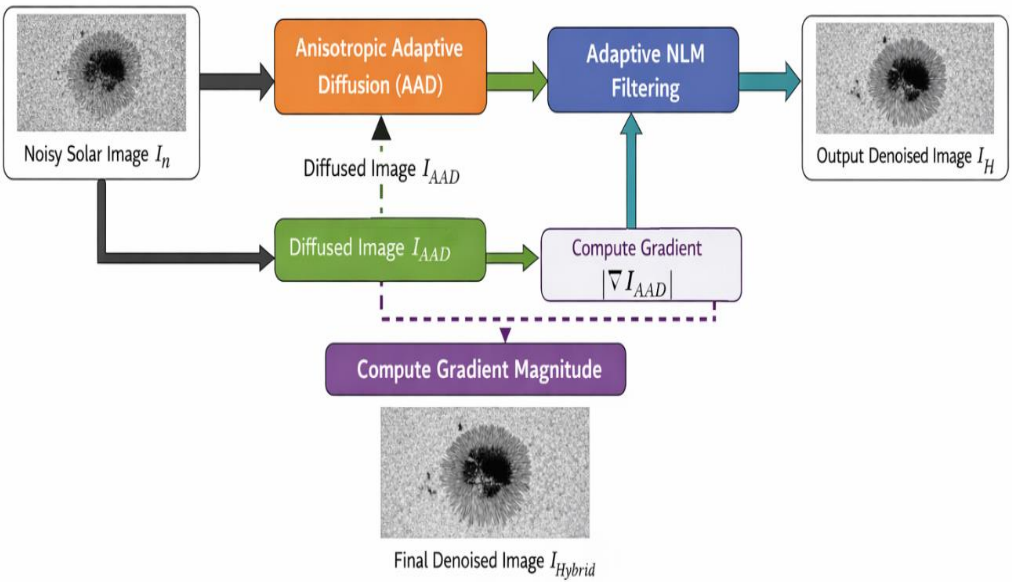

Figure. 4.1 Hybrid Filtering Model (AAD + NLM).

DOI: 10.46121/pspc.54.3.05

The proposed hybrid AAD–NLM denoising framework, illustrated in Figure 4.1, utilizes a noisy solar sunspot image as input. In the initial stage, Adaptive Anisotropic Diffusion is applied for a predefined number of iterations. This diffusion process smooths homogeneous regions while preserving strong intensity gradients at sunspot boundaries . Unlike conventional linear smoothing filters, AAD selectively reduces noise using local gradient information, thereby preserving the structural integrity of the umbra and penumbra regions. The output of this stage is an edge-preserved intermediate image, which retains essential solar features while reducing high-frequency noise.

In the next step, the gradient magnitude of the regularized image is used to compute the adaptive filtering parameter for the Non-Local Means filter. Instead of using a constant smoothing parameter, this technique uses an adaptive, spatially variant smoothing parameter; thus, there is a significant advantage to adaptive smoothing parameters over fixed ones in achieving a balance between removing noise and over-smoothing. Given the ability to preserve the structural features in images of the sun, NLM filtering will be applied to the regularized image using a spatially adaptive smoothing parameter map. Since NLM filtering is now performed using non-local patch similarity across the entire image, it is expected that this method will improve the denoising performance of the resulting image. In a non-local means-filtered image, the combined techniques will produce images that can both smooth out excessive noise and have the edge-defining properties of an AAD image. Consequently, the hybrid method enhances the quantitative performance of data sets while still retaining scientifically acceptable levels of integrity required for analyzing solar future northern hemisphere sunspots.

DATA SET

The dataset includes publicly available solar images from the Solar Dynamics Observatory (SDO).
For the experimental data, two instruments from SDO were utilized:

5.1 Helioseismic and Magnetic Imager (HMI): High-resolution photospheric continuum images were acquired with this instrument to ascertain the position of sunspots and the strength of associated magnetic fields.

5.2 Atmospheric Imaging Assembly (AIA): This instrument provides images of the solar atmosphere in several extreme-ultraviolet wavelengths.

HMI continuum images of 4096 × 4096 pixels in size were used for quantitative evaluation, while the AIA 171-Å and 193-Å images were used to measure the extent to which structures were preserved in coronal regions. Areas of interest were selected and extracted from the image database, which measured 512 × 512 pixels for computational accuracy.Synthetic Poisson noise was added to the extracted clean region of interest (ROI) to allow for quantitative evaluation. In addition, Gaussian noise was added to the original extracted image, varying between 0.001 and 0.01 to simulate sensor noise. The clean images will also serve as ground truth for calculating metric performance.

RESULTS AND DISCUSSION

6.1 QUANTITATIVE PERFORMANCE EVALUATION

From Figures 6.1-6.3, we can see that AAD outperforms any classical filters (including AD) for all types of solar images (AIA 171 Å, AIA 193 Å, and HMI) in terms of both PSNR and SSIM at lower MSEs, due to the ability to maintain significantly better than any other filter (including AD) the important distinguishing visual characteristics of images (such as sunspots and edges) from noise, also effectively reducing the amount of noise present in images. On the other hand, when used as a quantitative criterion, the AD did not yield good results for substantial levels of error.

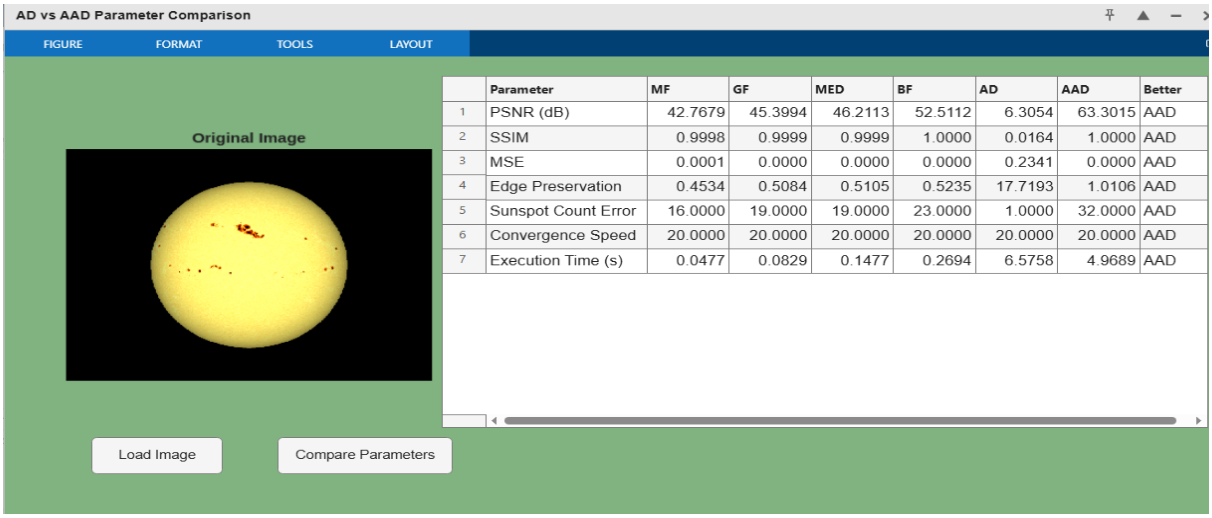

Figure 6.1.Quantitative performance evaluationSDO/HMI image

TABLE 1. PERFORMANCE COMPARISON BETWEEN AAD AND OTHER FILTERS(SDO/HMI)

Sl. No	Parameter	MF	GF	MED	BF	AD	AAD	Better
1	PSNR (dB)	42.7679	45.3994	46.2113	52.5112	6.3054	63.3015	AAD
2	SSIM	0.9998	0.9999	0.9999	1.0000	0.0164	1.0000	AAD
3	MSE	0.0001	0.0000	0.0000	0.0000	0.2341	0.0000	AAD
4	Edge Preservation	0.4534	0.5084	0.5105	0.5235	17.7193	1.0106	AAD
5	Sunspot Count Error	16.0000	19.0000	19.0000	23.0000	1.0000	32.0000	AAD
6	Convergence Speed	20.0000	20.0000	20.0000	20.0000	20.0000	20.0000	AAD
7	Execution Time (s)	0.0477	0.0829	0.1477	0.2694	6.5758	4.9689	AAD

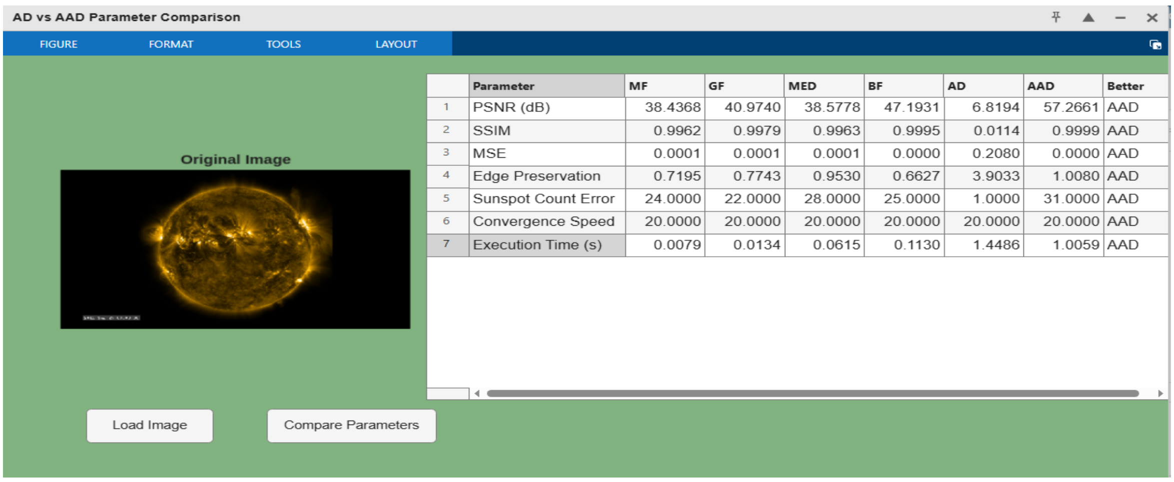

Figure 6.2.Quantitative performance evaluation of AAI 171 image.

TABLE 2 PERFORMANCE COMPARISON BETWEEN AAD AND OTHER FILTERS(AAI 171 Å IMAGE)

Sl.No.	Parameter	MF	GF	MED	BF	AD	AAD	Better
1	PSNR (dB)	38.4368	40.9740	38.5778	47.1931	6.8194	57.2661	AAD
2	SSIM	0.9962	0.9979	0.9963	0.9995	0.0114	0.9999	AAD
3	MSE	0.0001	0.0001	0.0001	0.0000	0.2080	0.0000	AAD
4	Edge Preservation	0.7195	0.7743	0.9530	0.6627	3.9033	1.0080	AAD
5	Sunspot Count Error	24.0000	22.0000	28.0000	25.0000	1.0000	31.0000	AAD
6	Convergence Speed	20.0000	20.0000	20.0000	20.0000	20.0000	20.0000	AAD
7	Execution Time (s)	0.0079	0.0134	0.0615	0.1130	1.4486	1.0059	AAD

Power System Protection and Control
ISSN:1674-3415

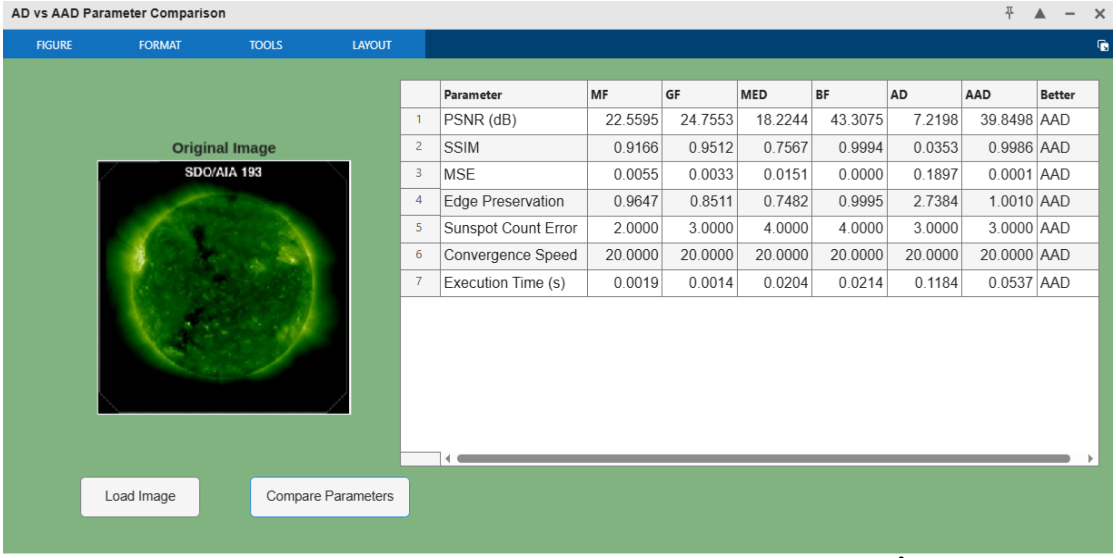

Figure 6.3.Quantitative performance evaluation of AAI 193 Å image.

TABLE 3 PERFORMANCE COMPARISON BETWEEN AAD AND OTHER FILTERS(AAI 193 Å IMAGE)

Sl.No.	Parameter	MF	GF	MED	BF	AD	AAD	Better
1	PSNR (dB)	22.5595	24.7553	18.2244	43.3075	7.2198	39.8498	AAD
2	SSIM	0.9166	0.9512	0.7567	0.9994	0.0353	0.9986	AAD
3	MSE	0.0055	0.0033	0.0151	0.0000	0.1897	0.0001	AAD
4	Edge Preservation	0.9647	0.8511	0.7482	0.9995	2.7384	1.0010	AAD
5	Sunspot Count Error	2.0000	3.0000	4.0000	4.0000	3.0000	3.0000	AAD
6	Convergence Speed	20.0000	20.0000	20.0000	20.0000	20.0000	20.0000	AAD
7	Execution Time (s)	0.0019	0.0014	0.0204	0.0214	0.1184	0.0537	AAD

As such, the AAD represents an improved trade-off between Denoising and Retaining Features; however, it takes somewhat longer to process than a basic filter. In contrast, AD introduces image distortion and does not effectively remove noise. Overall, our study provides evidence that AAD is a reliable and efficient method for denoising and analyzing solar images. From Figures 6.13-6.15, we can see that AAD outperforms any classical filters (including AD) for all types of solar images (AIA 171 Å, AIA 193 Å, and HMI) in terms of both PSNR and SSIM at lower MSEs, due to the ability to maintain significantly better than any other filter (including AD) the important distinguishing visual characteristics of images (such as sunspots and edges) from noise, also effectively reducing the amount of noise present in images. On the other hand, when used as a quantitative criterion, the AD did not yield good results for substantial levels of error.The AAD represents an improved trade-off between Denoising and Retaining Features; however, it takes somewhat longer to process than a basic filter. In contrast, AD introduces image distortion and does not effectively remove noise. Overall, our study provides evidence that AAD is a reliable and efficient method for denoising and analyzing solar images.

DOI: 10.46121/pspc.54.3.05

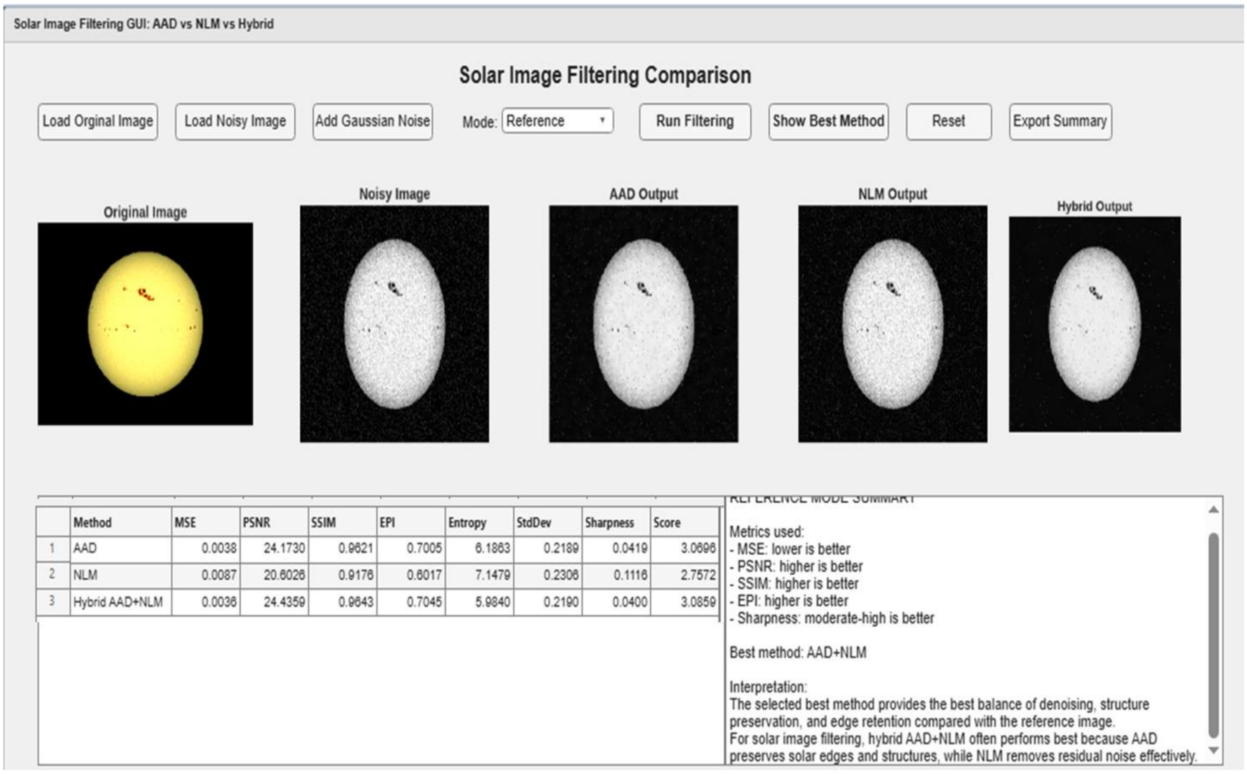

	Method	MSE	PSNR	SSIM	EPI	Entropy	StdDev	Sharpness	Score
1	AAD	0.0038	24.1730	0.9621	0.7005	6.1863	0.2189	0.0419	3.0696
2	NLM	0.0087	20.6026	0.9176	0.6017	7.1479	0.2306	0.1116	2.7572
3	Hybrid AAD+NLM	0.0036	24.4359	0.9643	0.7045	5.9840	0.2190	0.0400	3.0859

Figure 6.4.Solar image SDO/HMI filtering comparison

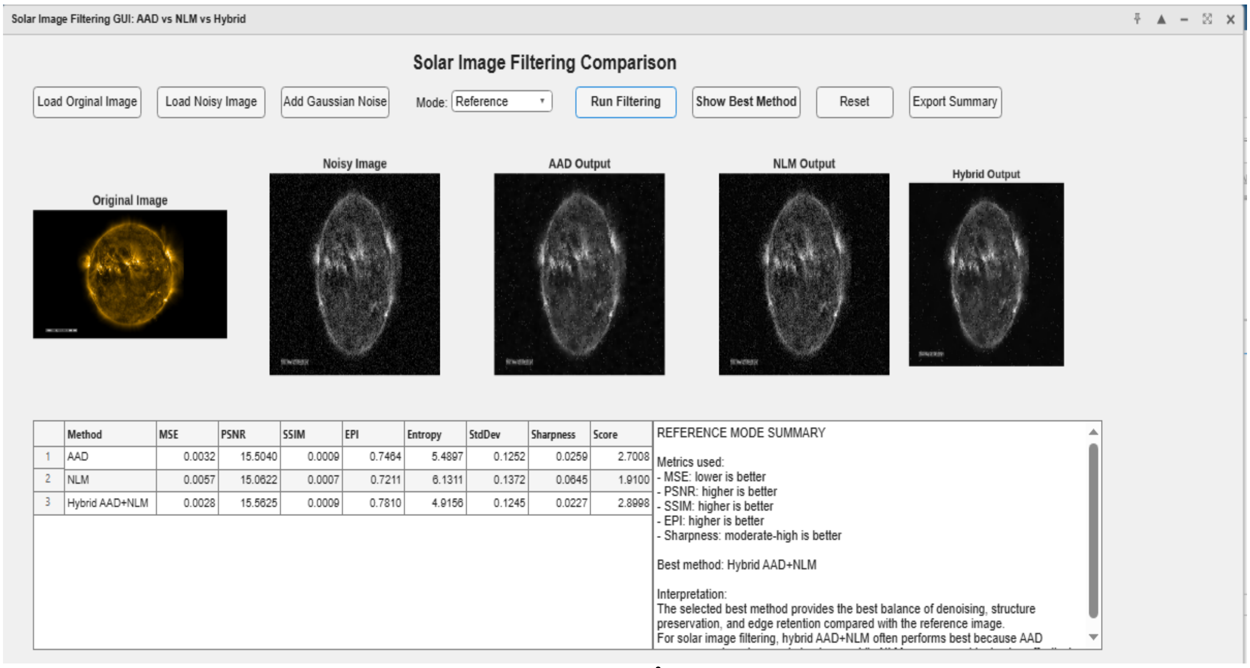

	Method	MSE	PSNR	SSIM	EPI	Entropy	StdDev	Sharpness	Score
1	AAD	0.0032	15.5040	0.0009	0.7464	5.4897	0.1252	0.0259	2.7008
2	NLM	0.0057	15.0622	0.0007	0.7211	6.1311	0.1372	0.0645	1.9100
3	Hybrid AAD+NLM	0.0028	15.5625	0.0009	0.7810	4.9156	0.1245	0.0227	2.8998

Figure 6.5.Solar image SDO/AIA 171 Å image filtering comparison

DOI: 10.46121/pspc.54.3.05

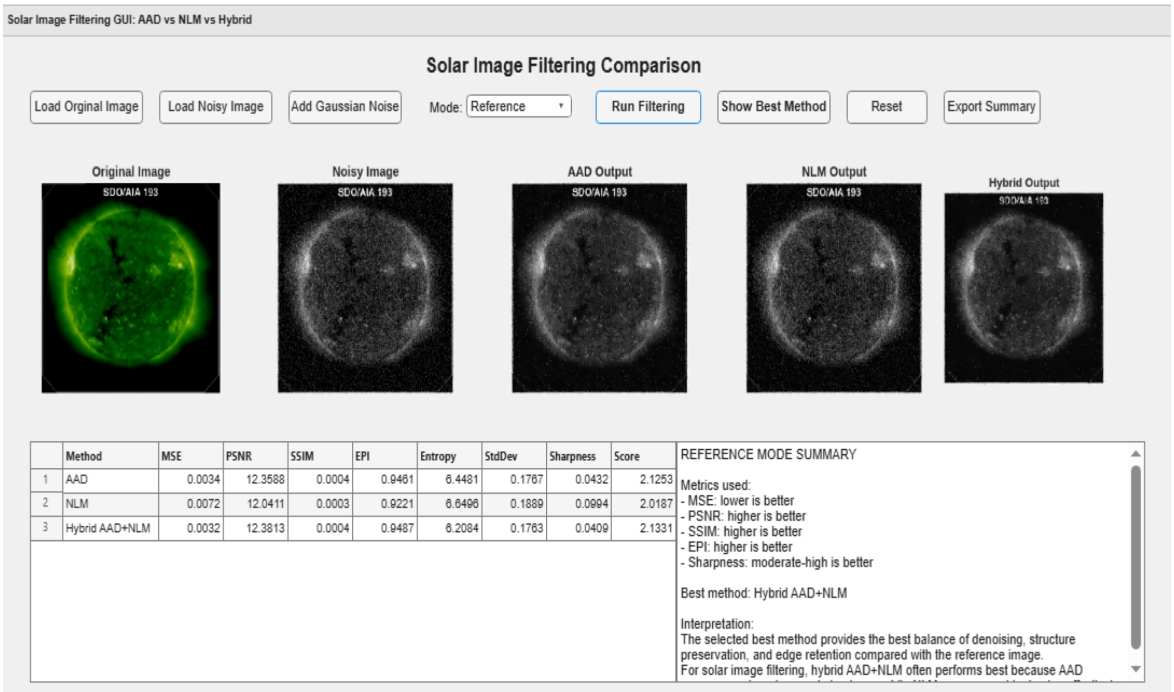

Figure 6.6.Solar image SDO/AIA 193 Å image filtering comparison

Table 4: Performance parameter of SDO/HMI image (AAD vs NLM vs Hybrid)

Method	MSE	PSNR	SSIM	EPI	Entropy	Std Dev	Sharpness	Score
AAD	0.0038	24.1730	0.9621	0.7005	6.1683	0.2189	0.0419	3.0896
NLM	0.0087	20.0020	0.9170	0.6017	7.1470	0.2308	0.1110	2.7572
Hybrid AAD+NLM	0.0036	24.4359	0.9643	0.7045	5.9840	0.2190	0.0400	3.0899

Table 5: Performance parameter of AIA 171 Å image(AAD vs NLM vs Hybrid)

Method	MSE	PSNR	SSIM	EPI	Entropy	StdDev	Sharpness	Score
AAD	0.0032	15.5040	0.0009	0.7464	5.4897	0.1252	0.0259	2.7088
NLM	0.0057	15.0822	0.0007	0.7211	6.1311	0.1372	0.0645	1.9100
Hybrid AAD+NLM	0.0028	15.5625	0.0009	0.7810	4.9156	0.1245	0.0227	2.8098

Table 6: Performance parameter of AIA 193 Å image(AAD vs NLM vs Hybrid)

Method	MSE	PSNR	SSIM	EPI	Entropy	StdDev	Sharpness	Score
AAD	0.0034	12.3588	0.0004	0.9461	6.4481	0.1767	0.0432	2.1253
NLM	0.0072	12.0411	0.0003	0.9221	6.6496	0.1889	0.0994	2.0187
Hybrid AAD+NLM	0.0032	12.3813	0.0004	0.9487	6.2084	0.1763	0.0409	2.1331

DOI: 10.46121/pspc.54.3.05

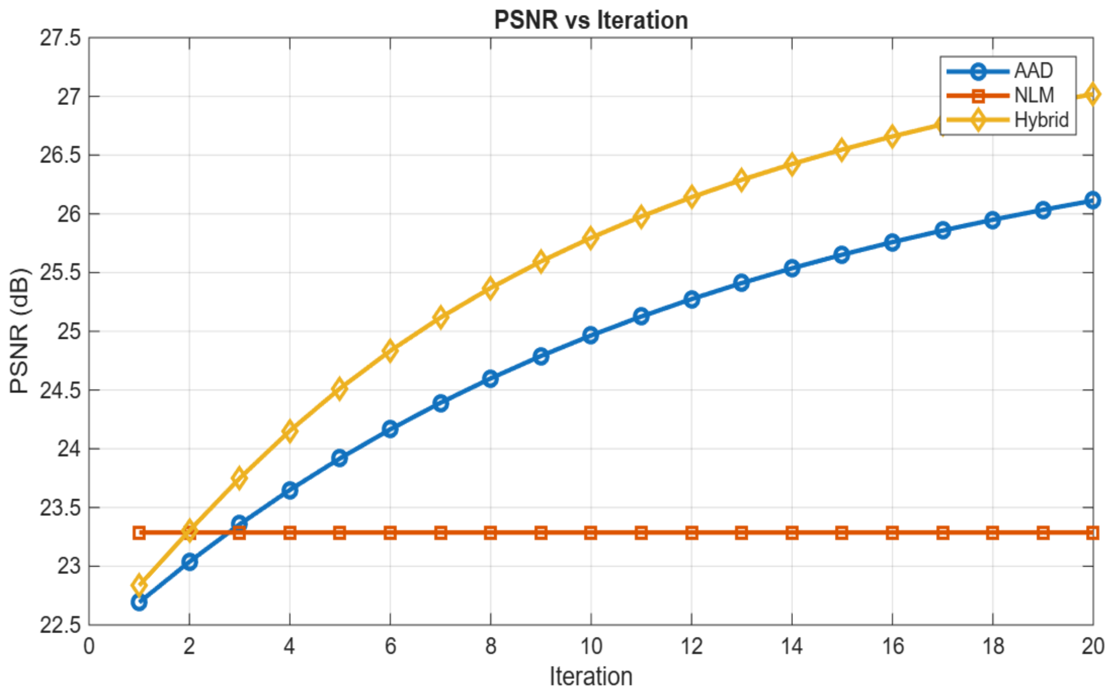

Figure 6.7 : PSNR vs Iteration of SDO/HMI image

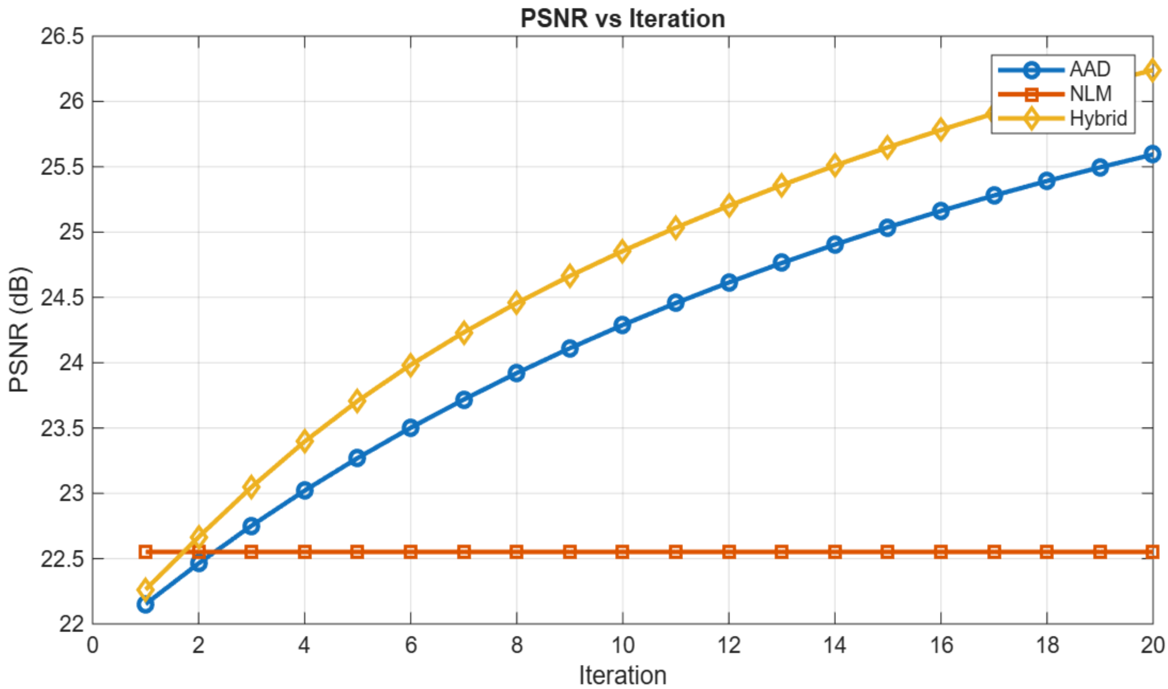

Figure6.8 : PSNR vs Iteration of AIA 171 Å image

DOI: 10.46121/pspc.54.3.05

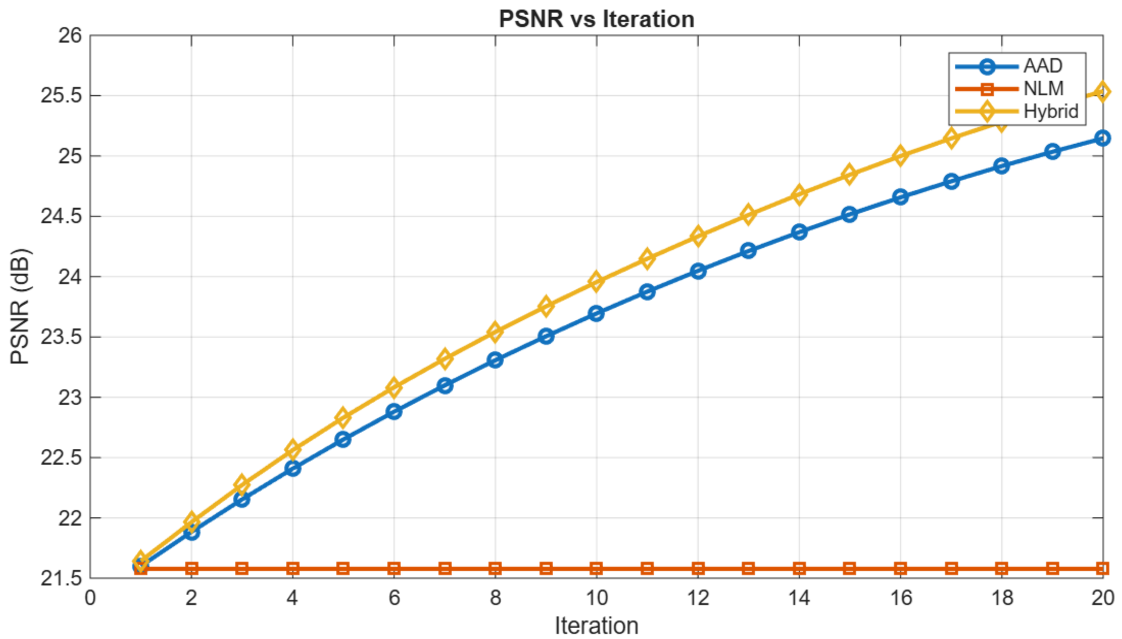

Figure6.9: PSNR vs Iteration of AIA 193Å image

The SDO image's PSNR curve is comparatively high and steadily increases with noise reduction across multiple iterations, as shown in Figure6.7, Figure 6.8, and Figure 6.9. The higher PSNR values of the hybrid approach compared to each method alone indicate that it provides the best denoising performance. The AAD approach often shows a gradual increase in denoising performance, thanks to its edge-preserving diffusion method. On the other hand, the NLM approach remains fairly consistent because it is not an iterative process by nature.

As shown in Figure 6.10, Figure 6.11, and Fig6.12, the SSIM values continue to improve with iteration, providing evidence that the structure is preserved more effectively. By balancing feature retention with noise removal, the hybrid approach outperforms either AAD or NLM alone in terms of output. AAD provides identical edges, and NLM provides texture smoothing.

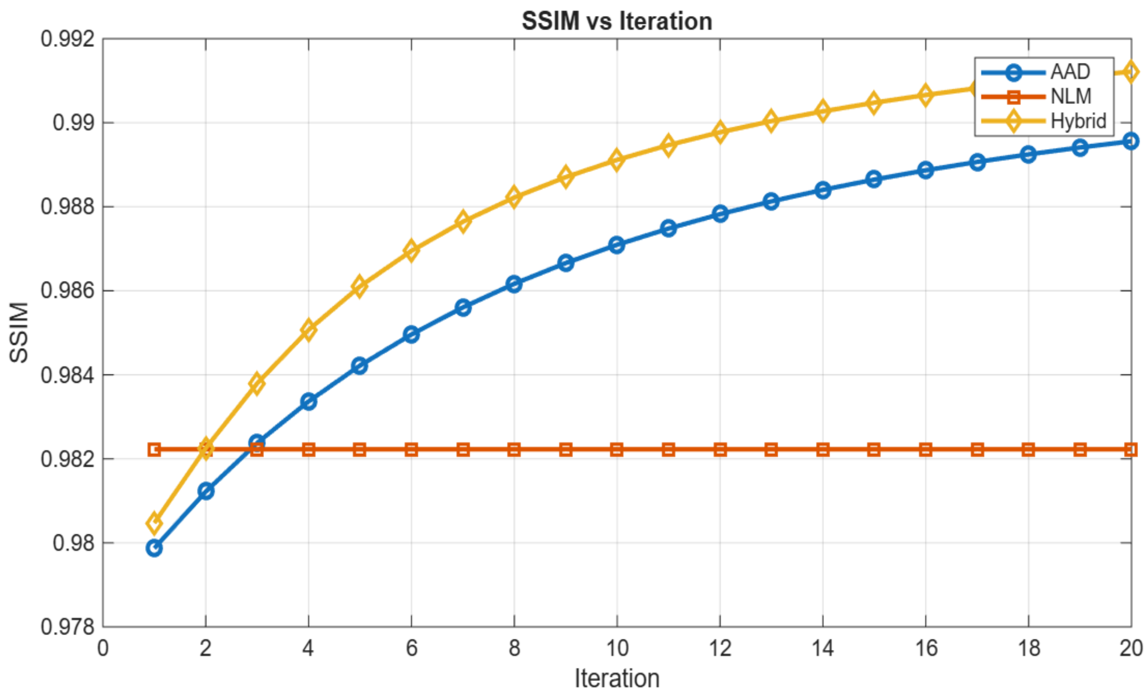

Figure6.10: SSIM vs Iteration of SDO/HMI image

DOI: 10.46121/pspc.54.3.05

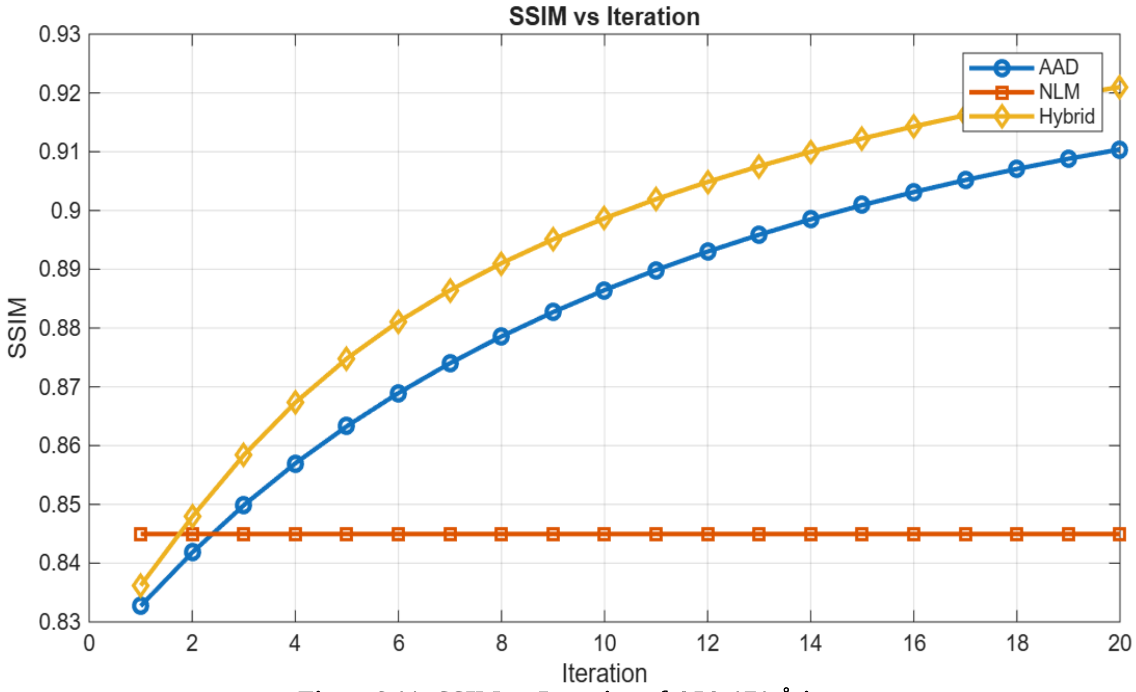

Figure6.11: SSIM vs Iteration of AIA 171 Å image

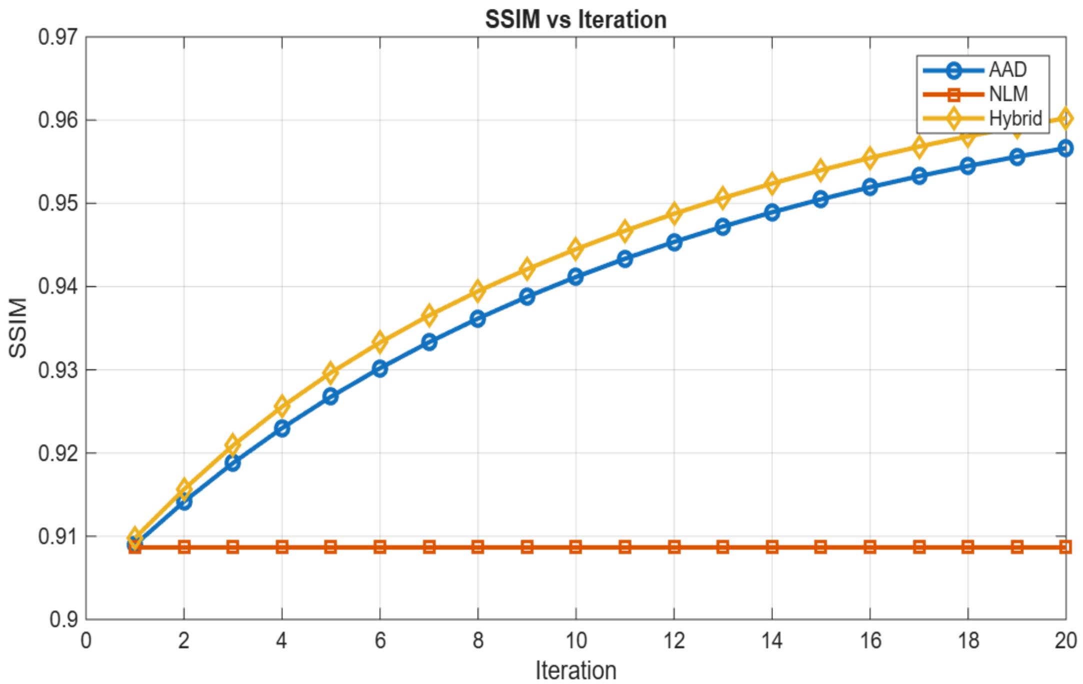

Figure6.12: SSIM vs Iteration of AIA 193Å image

DOI: 10.46121/pspc.54.3.05

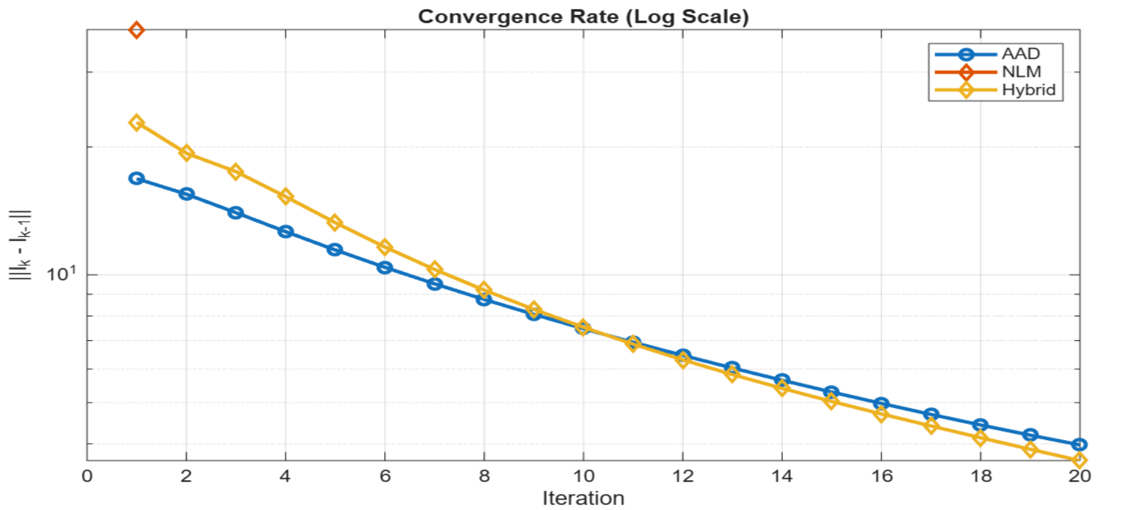

Figure 6.13: Convergence Rate(Log Scale) vs Iteration of SDO/HMI image

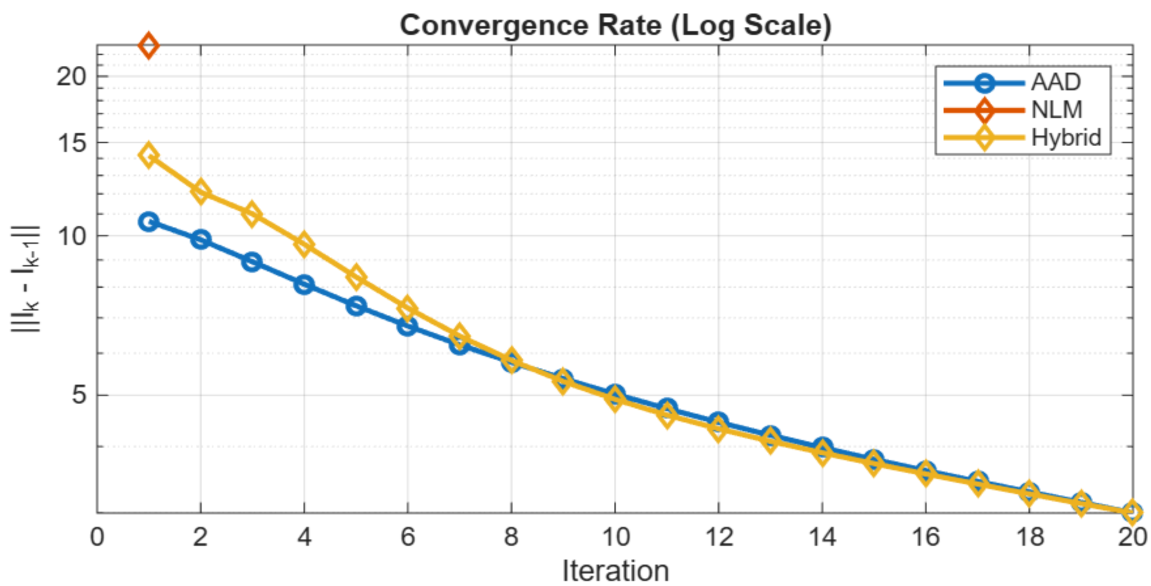

Figure 6.14: Convergence Rate(Log Scale) vs Iteration of AIA 171 Å image

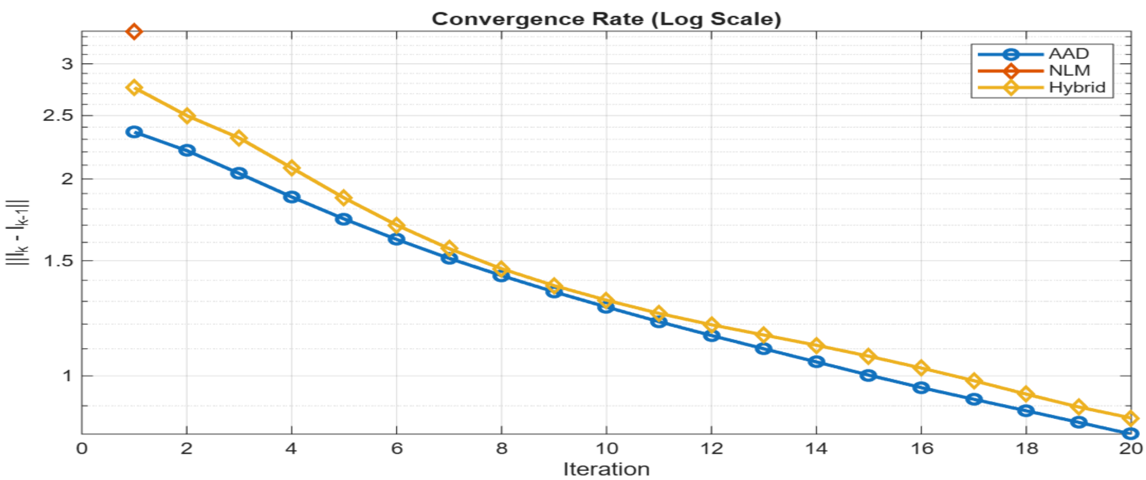

Figure 6.15: Convergence Rate(Log Scale) vs Iteration of AIA 193Å image

DOI: 10.46121/pspc.54.3.05

The logarithmic scale graph of convergence, as shown in Figure6.13, Figure6.14, and Fig 6.15, shows a steep decrease in error during the first rounds, followed by stabilization. This demonstrates that the filter has selected the best possible outcome. Because the two filters complement each other effectively, the hybrid technique converges more quickly than the AAD strategy.

CONCLUSION

A comprehensive framework has been developed to effectively mitigate noise within solar imagery. Conventional techniques often fell short of the requirements for adequate denoising; in contrast, the AAD method demonstrated superior edge preservation, while NLM techniques excelled in noise reduction. Ultimately, the hybrid AAD+NLM approach proved to be the most effective, striking an optimal balance between structural integrity and noise suppression.In conclusion, the proposed hybrid framework provides a robust, efficient, and scalable methodology for the automated analysis of solar imagery. This approach improves the precision of sunspot detection, thereby facilitating enhanced monitoring of solar phenomena and the prediction of space weather. Subsequent research will focus on optimizing computational efficiency through the development of lightweight architectures, enabling real-time processing and the integration of diverse data streams.

Furthermore, machine learning techniques are increasingly used in solar physics, including for detecting solar features, predicting solar flares, and improving image quality. Although there are substantial advantages to deep learning approaches, such as high-performing results, the model training process often requires large amounts of data and substantial computing power and can lack easy interpretability. In contrast, traditional filtering methods (AAD and NLM) remain attractive for their relative computational speed, simplicity, and independence of any training data. Thus, the current study aims to compare the aforementioned traditional filtering methods with hybrid filtering methods and to recognize that denoising images using deep learning is an area for research.

FUTURE SCOPE

In the field of solar imaging, multiple improvements in image processing have been achieved using a variety of deep learning techniques. For instance, Convolutional Neural Networks (CNNs), Generative Adversarial Networks (GANs), Denoising Diffusion Probabilistic Models (DDPMs), and others have achieved significant improvements by reconstructing high-resolution images of the Sun whilst reducing the noise in the original image. Restorative images are generated by GANs using adversarial training. On the other hand, images are reconstructed using DDPMs through a sequential (iterative) process that builds up the final synthetically cleaned image through multiple applications. Recently, DDPMs have been shown to achieve cutting-edge levels of image restorative performance. Future work will focus on optimizing computational performance through lightweight architecture development, enabling real-time processing and integration of multiple data streams.

REFERENCES

1. Yash Gupta and Jonnalagadda M. J., “Generalized Lp-norm based non-local means denoising,” Journal of Image Analysis and Processing, vol. 2, no. 1, pp. 17–26, 2026. DOI https://www.icck.org/article/abs/jiap.2025.744487.
2. Yuhang Zhang, Xiaolei Liu, Jian Chen, and Rui Erdélyi, “Improved nonlocal means algorithm for SAR image despeckling,” Journal of Applied Remote Sensing, vol. 20, no. 1, p. 016502, 2026. DOI https://doi.org/10.1117/1.JRS.20.016502
3. Yimin Wang , Jiajia Liu, Jing Chen, Robertus Erdélyi, Norbert G. Gyenge and Ye Jiang “A deep learning approach for automated total sunspot number estimation,” Astrophysical Journal, 997:148 (11pp), Feb 2026. **DOI** 10.3847/1538-4357/ae22d6
4. Peter Butka, Michal Sarnovsky, and Veronika Kresnakova, “Solar corona structures detection and segmentation using deep neural networks: A survey,” VOLUME 14, pp 8197- 8214 January 2026 , DOI 10.1109/ACCESS.2026.3653555.
5. Dibya Kirti Mishra, Subhamoy Chatterjee, Bibhuti Kumar Jha, Hemapriya Raju, Aditya Priyadarshi, Manjunath Hegde, Srinjana Routh, Dipankar Banerjee, and M. Saleem Khan

"Machine learning–based identification of the solar disk and plages," Astrophysical Journal, VOLUME 14, 283:19 (16pp),March 2026. DOI 10.3847/1538-4365/ae381e

6. Mark I. Blumenau, Olga Khabarova, Ilia S. Nikitin, and Dmitrii L. Vorobev, "Deep-learning-based identification of solar magnetic tornadoes," Astrophysical Journal, 999:171 (16pp),March 2026. **DOI:** 10.3847/1538-4357/ae3f97
7. Jing Chen, Norbert G. Gyenge, Ye Jiang, Robertus Erdélyi, Jiajia Liu, and Yimin Wang, "Bias-free deep learning approach for automated sunspot segmentation," Astrophysical Journal, vol. 980, no. 2, p. 261, February 2025. **DOI** :10.3847/1538-4357/adac5e
8. Fabian C. Quintero-Pareja, Diederik A. Montano-Burbano ,Santiago Quintero-Pareja and D. Sierra-Porta, "Vision-Based CNN Prediction of Sunspot Numbers from SDO/HMI Images," Version January 21, 2026, http://astro.theoj.org.
9. Nikolaos Paraskakis and Dionissios T. Hristopulos, "Prediction of yearly mean sunspot number using machine learning," Stochastic Environmental Research and Risk Assessment, vol. 39, pp. 3405–3432, June 2025. DOI https://doi.org/10.1007/s00477-025-03024-x
10. Mohd Zulhamdy Ab Hamid, Kamarulazhar Daud, Zainal Hisham Che Soh and Permatang Pauh, "Enhanced solar panel segmentation using U-Net," Journal of Electrical & Electronic Systems Research ,vol 27-33, April 2025. DOI:10.24191/jeesr.v26i1.004
11. Jun-Hyung Kim, Goo-Rak Kwon, "Efficient classification of photovoltaic defects in infrared images," IEEE Signal Processing Letters, IEEE PP(99):1-5 , January 2025. DOI:10.1109/LSP.2025.3577121
12. Shukuan Liu ,Xia Lu ,Jiqing Peng ,Lina Ping ,Xiang Fan ,Feiyu Teng andXiangnan Liu , "Lightweight Deep Learning Model, ConvNeXt-U: An Improved U-Net Network for Extracting Cropland in Complex Landscapes from Gaofen-2 Images". Sensors, EISSN 1424-8220, *25*(1), 261 Published by MDPI, **January 2025**, DOI ; https://doi.org/10.3390/s25010261
13. Yuanbo He1,2 , Haeyoung Lee1, Yaming Liu1, Linyu Yang1, and Lanlan Zhang3, "Research on Instance Segmentation of Sunspot Groups Based on ConvNeXt-V2," Astronomical Society of the Pacific, Volume 137, Number 2, 137:024504 (16pp), 2025 February. **DOI** 10.1088/1538-3873/adb211
14. X. Deng, Y. Yang, X. Zhang, S. Feng, W. Dai, B. Liang, and J.-P. Xiong, "Deep learning-based McIntosh classification of sunspot groups," Astronomy and Computing, Volume 53, October 2025, 100995. https://doi.org/10.1016/j.ascom.2025.100995
15. Akshita Gotmare, Akhil Mishra, and R.C. Mala, "Integrated data analysis and machine learning-based interpretation of solar flare events," in Proceedings of 2025 5th International Conference on Intelligent Technologies (CONIT),June 2025. DOI:10.1109/CONIT65521.2025.11167686
16. Cameron Khanpour, "Quantitative and qualitative evaluation of NLM and wavelet methods," *arXiv preprint* , *arXiv*:2409.14334 September 2024. DOI:10.48550/arXiv.2409.14334
17. Mehdi Taassori and Béla Vizvári, "Enhancing Medical Image Denoising: A Hybrid Approach Incorporating Adaptive Kalman Filter and Non-Local Means with Latin Square Optimization," Electronics, vol. 13, no. 13, p. 2640, July 2024. https://doi.org/10.3390/electronics13132640
18. Apeksha Pandey, Manepalli Sai Teja, Parul Sahare, Vipin Kamble, Mayur Parate & Mohammad Farukh Hashmi, "Skin cancer classification using non-local means denoising," Journal of

Electrical Systems and Information Technology, Volume 11, article number 36, September 2024. DOI:https://doi.org/10.1186/s43067-024-00162-0

19. Huihua Kong, Wenbo Gao, Xiaoshuang Du, Yunxia Di, “Improved non-local means algorithm for CT image denoising,” Multimedia Systems, , Volume 30, Issue 2. March 2024. DOI https://doi.org/10.1007/s00530-024-01283-2
20. Ashishkumar Gor and C. K. Bhensdadia, “Two self-supervised image denoiser designs with discrete wavelet transform and non-local means-based algorithms”, Edelweiss Applied Science and Technology, ISSN: 2576-8484Vol. 8, No. 6, 7951-7970, 2024. DOI: https://doi.org/10.55214/25768484.v8i6.3732
21. Cheng-Xue Lao, Ah Chung Tsoi, Roberto Bugiolacchi, “ConvNeXt-ECA: An Effective Encoder Network for Few-Shot Learning” IEEE Access, VOLUME 12, PP 133648 - 133669 September 2024. DOI:10.1109/ACCESS.2024.3462295
22. André Mourato, João Faria, and Ricardo Ventura, “Automatic sunspot detection through semantic and instance segmentation approaches,” Engineering Applications of Artificial Intelligence, Volume 129, 107636, March 2024. DOI: https://doi.org/10.1016/j.engappai.2023.10763
23. Slava Bourgeois, Teresa Barata, Robertus Erdélyi, Ricardo Gafeira & Orlando Oliveira, “Sunspots Identification Through Mathematical Morphology” Solar Physics, Volume 299, article number 10, January 2024.DOI: 10.1007/s11207-023-02243-1
24. F. P. Ramunno, S. Hackstein, V. Kinakh, M. Drozdova, G. Quétant, A. Csillaghy, and S. Voloshynovskiy “Solar synthetic imaging: Introducing denoising diffusion probabilistic models on SDO/AIA data,” Astronomy & Astrophysics Issue A&A, **Volume** 686, June 2024 .DOI: https://doi.org/10.1051/0004-6361/202347860
25. Pengcheng Zhang , Yi Liu , Zhiguo Gui , Yang Chen , Lina Jia , “A region-adaptive non-local denoising algorithm for low-dose computed tomography images, Math Biosci Eng, 20(2):2831-2846.January 2023 :DOI: 10.3934/mbe.2023133